ADVANCED MATERIALS
www.advmat.de

Epitaxial Ultrathin Organic Crystals on Graphene for High-Efficiency Phototransistors

Xiaolong Liu, Xiaoguang Luo, Haiyan Nan, Hui Guo, Peng Wang, Linglong Zhang, Minmin Zhou, Ziyi Yang, Yi Shi, Weida Hu, Zhenhua Ni, Teng Qiu,* Zongfu Yu, Jian-Bin Xu, and Xinran Wang**

Organic small molecules and polymers are important class of materials for photodetector applications, offering wide material selection, excellent mechanical flexibility, and roll-to-roll manufacturing capability.[1–3] The energy gap of organic semiconductors (OSCs) can cover the entire spectral range from near infrared to ultraviolet (UV).[4] However, the short exciton diffusion length and low mobility in organic materials post severe challenges in achieving high efficiency and short response time. Interfacing OSCs with other materials can alleviate this problem. One way is to fabricate organic bulk heterojunctions, where the charge-transfer states at the donor–acceptor interface can facilitate charge separation.[5,6] Even then, the charge carriers still need to transport in a low-mobility material for extended length scale to be collected. Another way is to interface OSCs with high mobility materials such as graphene to create sensitized organic phototransistors (OPTs).[7–12] This device structure can, in principle, combine the optical-spectral-sensitivity of OSCs and mobility of graphene to afford ideal OPTs with high quantum efficiency (QE) and bandwidth. Here, the device performance critically depends on the microscopic structure and quality of OSCs near the interface, which is the locus for exciton dissociation.[8] However, previous studies on organic/graphene hybrid phototransistors mainly used solution-processed OSCs without any knowledge or control of the interface quality.[7–11] This could lead to severe underperformance of the phototransistors. In principle, the thickness of the OSCs should be less than the exciton diffusion length, which is on the order of 10 nm,[1] to achieve the highest charge separation efficiency.

Recently, we have demonstrated van der Waals (vdW) epitaxy of ultrathin organic crystals on graphene and boron nitride (BN) for electronic device applications.[13,14] The nearly ideal interface afforded record-high mobility in monolayer OSCs and band-like transport. Herein, by utilizing dioctylbenzothienobenzothiophene (C_8-BTBT) small molecule as an example, we explore ultrathin epitaxial OSC on graphene for high-efficiency OPTs. We observe prominent photoresponses even in the limit of monolayer C_8-BTBT (less than 3 nm), with photoresponsivity (R) up to 1.57×10^4 A W^{-1}, short response time of 25 ms and photoconductive gain (G_{ph}) over 10^8. Furthermore, sequential epitaxial growth of C_8-BTBT allows us to study the evolution of OPT performance. We observe a linear increase of external QE (EQE) as a function of increasing C_8-BTBT thickness up to approximately seven layers. For few-layer C_8-BTBT/graphene OPTs, the interfacial charge transfer efficiency (η_{trans}) and G_{ph} reach up to 41% and 1.84×10^9, respectively, which are among the highest in graphene-based photodetectors. The increase of EQE in thicker C_8-BTBT devices is accompanied by longer response time in the carrier recombination process, due to the greater energy barrier hopping between C_8-BTBT layers. The response of phototransistors with monolayer C_8-BTBT can be more than 30 times faster than multilayers. Our work provides important insights toward rational design of high-performance hybrid OPTs.

To fabricate the C_8-BTBT/graphene hybrid OPTs, we epitaxially grew C_8-BTBT layers on prepatterned graphene field-effect transistors (FETs) with Au electrodes in a home-built chemical vapor deposition (CVD) furnace.[13] Briefly, we placed the C_8-BTBT powder (provided by Nippon Kayaku Co., Ltd. Japan without further purification) at the center of the furnace and the graphene devices downstream. We evacuated the furnace to about 1×10^{-4} Torr and heated up the source to ≈110 °C to start growth. The thickness of the C_8-BTBT layers could be well controlled by tuning the evaporation temperature, growth time,

Dr. X. Liu, L. Zhang, M. Zhou, Z. Yang, Prof. Y. Shi, Prof. X. Wang
National Laboratory of Solid State Microstructures
School of Electronic Science and Engineering
Collaborative Innovation Center
of Advanced Microstructures
Nanjing University
Nanjing 210093, China
E-mail: yshi@nju.edu.cn; xrwang@nju.edu.cn
X. Luo, H. Nan, Prof. Z. Ni, Prof. T. Qiu
Department of Physics
Southeast University
Nanjing 211189, China
E-mail: tqiu@seu.edu.cn
X. Luo, Prof. Z. Yu
Department of Electrical and Computer Engineering
University of Wisconsin-Madison
Madison, WI 53706, USA
Prof. H. Guo
School of Microelectronics
Xidian University
Xian 710071, China
P. Wang, Prof. W. Hu
National Laboratory for Infrared Physics
Shanghai Institute of Technical Physics
Chinese Academy of Sciences
500 Yu Tian Road, Shanghai 200083, China
Prof. J.-B. Xu
Department of Electronic Engineering and Materials Science and Technology Research Center
The Chinese University of Hong Kong
Hong Kong SAR, China

DOI: 10.1002/adma.201600400

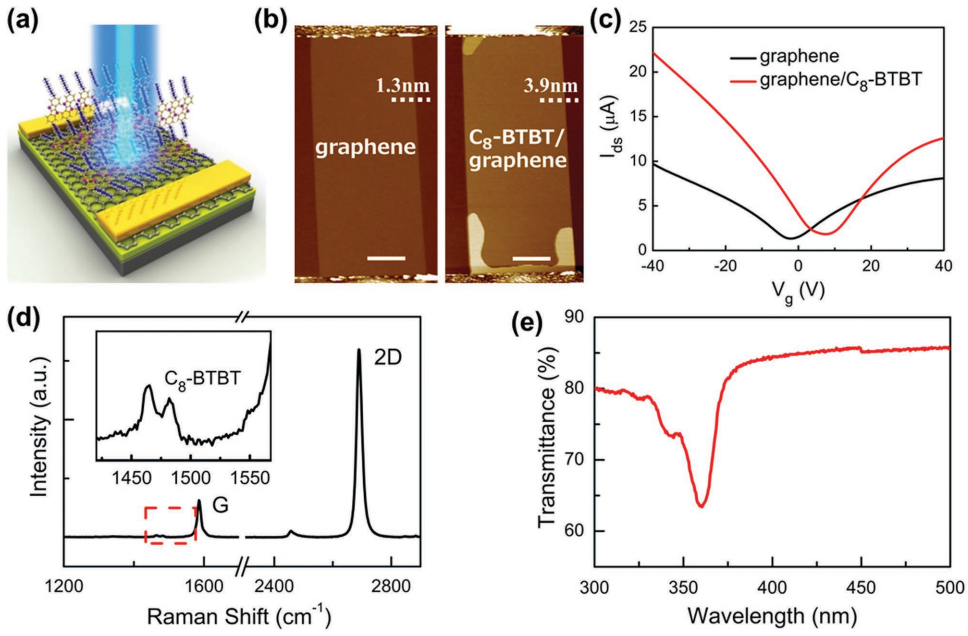

Figure 1. Characterization of epitaxial C_8-BTBT/graphene phototransistors. a) Schematic illustration of a typical phototransistor. b) The AFM images of a graphene FET before (left) and after (right) C_8-BTBT epitaxial growth. The device is mostly covered by IL + 1L C_8-BTBT as reflected from the measured height increase by 2.6 nm. Scale bars, 2 μm. c) Transfer characteristics of the graphene device in (b), before (black) and after (red) deposition of C_8-BTBT. d) Raman spectrum of ultrathin C_8-BTBT on graphene. The two prominent peaks are *G* and 2D peaks from graphene. Inset shows the magnified view near 1500 cm^{-1}, clearly showing the Raman signature of C_8-BTBT. e) Optical transmission spectrum of C_8-BTBT on quartz substrate. The absorption peak is at 360 nm.

and the position of the substrate. The mobility of the graphene transistors prior to C_8-BTBT deposition is typically on the order of 5000 cm^2 V^{-1} s^{-1}. **Figure 1** shows the schematic and atomic force microscopy (AFM) image of a representative OPT. Over 90% of the graphene was uniformly covered by the interfacial layer (IL) and the first layer (1L) of C_8-BTBT, as reflected by height increase by 2.6 nm (Figure 1b).[13] A small portion of the second layer (2L) appeared near the corners with the height of 3 nm. The growth of C_8-BTBT on graphene was further confirmed by Raman spectroscopy (Figure 1d).

C_8-BTBT is a wide bandgap OSC with absorption peaked at 360 nm (Figure 1e).[15] In this work, we used a 355 nm laser with 2 mm spot size to study the photoresponses of the hybrid OPTs. The laser power was carefully tuned below the damage threshold of the C_8-BTBT due to excessive heating. All the optoelectronic measurements were performed in a vacuum probe station to avoid the doping effect of ambient absorbents. Both static (Figure S1b, Supporting Information) and dynamic (with a chopper) measurements were performed with consistent results (see the Supporting Information for details). We thus focus the discussion on dynamic measurements, which also provide information on device response time and photoconductive gain. As expected, pure graphene devices with symmetric contacts did not show apparent photoresponses due to weak absorption (**Figure 2**b, top panel).[16–19] After epitaxial growth of C_8-BTBT, the charge neutrality point (CNP) of graphene (measured in vacuum) shifted toward positive voltages (Figure 1c), indicating that electrons were transferred from graphene to C_8-BTBT, creating an interfacial built-in field as shown in the inset of Figure 2c. Sequential growth of thicker C_8-BTBT could lead to further shift of the CNP (Figure S1a, Supporting Information). Under laser illumination, the built-in field was responsible for separating electron–hole pairs in C_8-BTBT, with electrons (holes) moving toward graphene (C_8-BTBT). As a result, the graphene became n-doped under illumination (Figure S1b, Supporting Information), giving rise to the observed photoresponse.

We first studied IL C_8-BTBT/graphene OPTs but unexpectedly observed very weak and slow photoresponse (Figure S2, Supporting Information). Such behavior points to low charge separation efficiency in IL, which is not well understood. One possible explanation is that holes in IL C_8-BTBT can easily recombine with electrons in graphene because of their close proximity (≈0.5 nm). Another possible reason is the substrate screening effect, which can strongly modulate the electronic properties of monolayer OSCs including the energy gap between the highest occupied molecular orbital (HOMO) and the lowest unoccupied molecular orbital (LUMO).[20] In the rest of the paper, we do not count IL when calculating the number of C_8-BTBT layers because of its trivial contribution to the photoresponse. Since thicker samples can be less uniform, we use the average number of C_8-BTBT layers (calculated as the total area of C_8-BTBT monolayers on graphene divided by the area of graphene channel) to describe the thickness.

Figure 2b (top panel) shows typical dynamic photocurrent (I_{ph}) response of a hybrid OPT with nearly monolayer C_8-BTBT under bias voltage V_{ds} = 0.1 V. The device has short response time $\tau \approx 20$ ms in both carrier separation (laser on) and recombination (laser off) processes. The latter is over one order of magnitude faster than similar devices with solution processed

Adv. Mater. **2016**,
DOI: 10.1002/adma.201600400

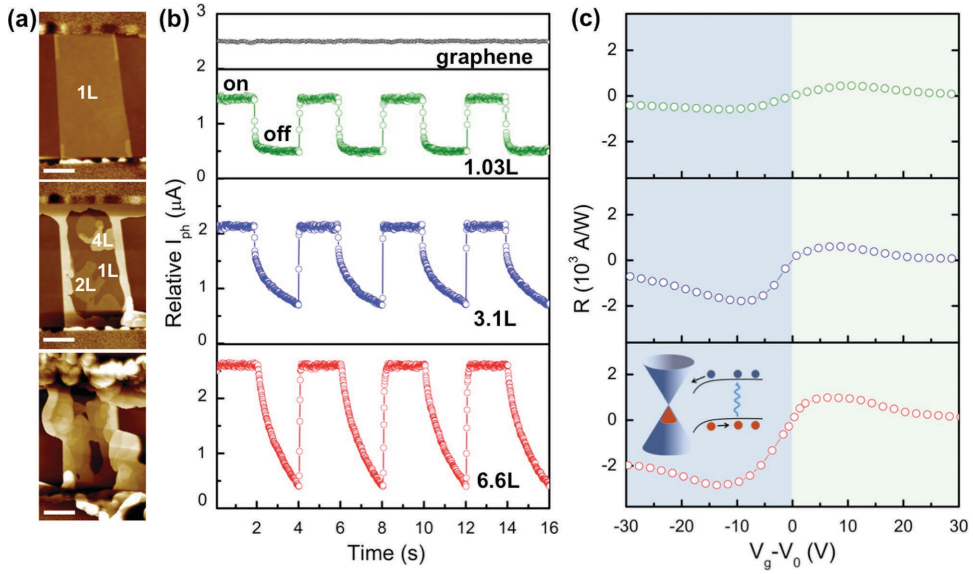

Figure 2. Photoresponse of hybrid C_8-BTBT/graphene phototransistors and the evolution with increasing C_8-BTBT thickness. a) AFM images of the same device undergone repeated C_8-BTBT growth. From top to bottom, the average number of C_8-BTBT layers is 1.03, 3.1, and 6.6, respectively. Scale bars, 2 μm. b) The dynamic photocurrent response of the devices in (a) under the same experimental conditions: laser power density: 7000 μW cm^{-2}, V_{ds} = 0.1 V, $V_g - V_0$ = 10 V. The top panel shows the photocurrent response of pure graphene device without C_8-BTBT. c) Measured photo responsivity as a function of V_g of the devices in (a) under the same experimental conditions: laser power 7000 μW cm^{-2}, V_{ds} = 0.1 V. The inset in the bottom panel shows the band structure and carrier transport under laser illumination.

OSCs.[7–9] The responsivity, $R = I_{ph}/P_{in}$, shows a strong modulation by gate voltage (V_g) with a change of sign near $V_g = V_0$ (Figure 2c), which corresponds to the cross point between the transfer curves under dark and illumination (Figure S1b, Supporting Information). When $V_g < V_0$, the conduction in graphene is dominated by holes. Under laser illumination, the injection of electrons from C_8-BTBT effectively decreases the carrier concentration and results in a negative R. When $V_g > V_0$, on the other hand, the concentration of carriers (in this case electrons) increases under illumination, resulting in a positive R.[21–23] The maximum R on both sides corresponds to the peak mobility in the underlying graphene. We also observed a power-law dependence of R on laser power (**Figure 3**a). For nearly monolayer samples, R could be as high as 1.57×10^4 A W^{-1} (under V_{ds} = 0.1 V, unless otherwise stated). The responsivity is at least two orders of magnitude higher than traditional vapor or solution processed low-mobility UV OPTs.[1] For organic single crystals UV OPT, only single crystal compound, which consist of anthracene core and contain two 2-ethynyl-5-hexyl-dithieno thiophene (A-EHDTT) groups in the 9,10-positions of the anthracene core, showed similar responsivity, but with much longer response time $\tau \approx 15$ s.[24] Considering that the photon-absorbing layer consists of monolayer molecules, the charge separation efficiency of our devices should be significantly higher. Long-term stability is also an important issue in organic devices. To test the stability, we measured the same OPT as fabricated and one month later (Figure S3, Supporting Information). Both topography and photoresponse measurements (including responsivity and response time) did not show appreciable change, indicating that our devices had excellent long-term stability despite the molecularly-thin nature of C_8-BTBT.

The controlled layer-by-layer vdW epitaxy enables us to study the evolution of key device metrics as a function of OSC thickness and morphology. This aspect is illustrated in Figure 2, where we compare the same device with nearly monolayer (top panels) and few-layer (middle and bottom panels) C_8-BTBT as the photon-absorbing layer. As the C_8-BTBT layers became thicker, we observed the increase of both responsivity and response time (mainly in the recombination process) under the same experimental conditions (Figure 2b,c). This trend was reproducible in all the devices undergone repeated growths (Figure 3a and Figure S4–S6, Supporting Information). In few-layer devices, R could reach 4.76×10^5 A W^{-1}. This is, to the best of our knowledge, the highest responsivity for organic UV photodetectors in any configurations.[1] We note that the responsivity does not saturate yet (Figure 3a), so higher responsivity is expected under even lower laser power. Currently, the maximum R is limited by the noise of our electrical measurement setup. Alternatively, one could use C_8-BTBT/graphene/BN structure to increase the mobility of graphene for better performance.[25]

We further analyze the EQE of our hybrid OPTs by $\mathrm{EQE} = \frac{I_{ph}}{q\phi_{in}} = RE_{ph}/q$, where ϕ_{in} is the incident photon flux, q is the elemental charge, and E_{ph} is the photon energy.[26] Typical EQE of the hybrid OPTs is on the order of 10^4 and 10^6 for monolayer and thicker C_8-BTBT, respectively (Figure 2a). The EQE is much higher than unity due to the large photoconductive gain in our sensitized phototransistors,[26] as will be discussed later. Figure 3b shows the EQE as a function of average number of C_8-BTBT layers under the same laser power of 100 μW μm^{-2} for all the measured devices. The roughly linear relationship up to approximately seven layer suggested that excitons in the top

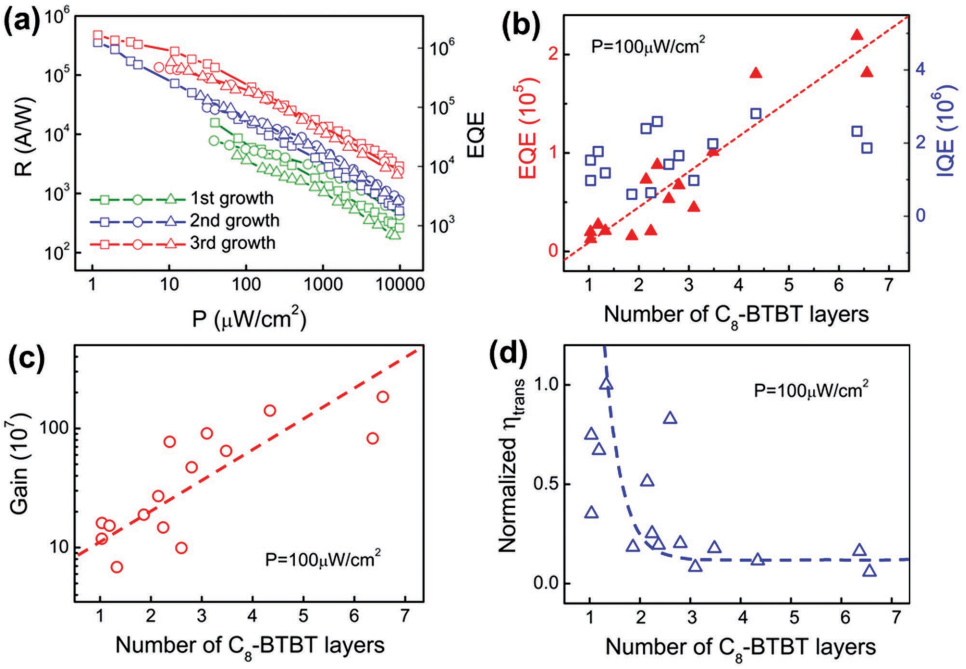

Figure 3. Device performance of hybrid C_8-BTBT/graphene phototransistors. a) Photo responsivity and EQE as a function of laser power density for three sets of devices (represented by squares, circles, and triangles, respectively) that have undergone repeated C_8-BTBT growths. The average numbers of C_8-BTBT layer are within 1L–2L, 2L–4L and 4–7L after the first, second and third growth, respectively. b) EQE (red triangles) and IQE (blue squares) as a function of average number of C_8-BTBT layers for all the measured devices (laser power, 100 μW cm^{-2}). The red dashed line reflects the linear increase of EQE. c) Photoconductive gain (G_{ph}) as a function of average number of C_8-BTBT layers for all the measured devices (laser power, 100 μW cm^{-2}). The red dashed line reflects the exponential increase of G_{ph}. d) Normalized η_{trans} (laser power, 100 μW cm^{-2}) as a function of C_8-BTBT thickness. The blue dashed line reflects the exponential decrease of η_{trans}. All the data are extracted under the gate voltage that gives the maximum responsivity in the $V_g - V_0 < 0$ regime.

C_8-BTBT layers could still diffuse to the interface and dissociate efficiently, implying an exciton diffusion length of at least ≈20 nm. The internal quantum efficiency (IQE) could be calculated as $\mathrm{IQE} = \frac{\mathrm{EQE}}{\eta_{abs}} = \frac{\mathrm{EQE}}{1-\exp(-ax)}$,[27] where $\eta_{abs} = 1-\exp(-ax)$ is the optical absorption for C_8-BTBT film with thickness x and absorption coefficient α. To this end, we deposited C_8-BTBT with different thickness on quartz substrates and measured the absorption at 355 nm (Figure S7, Supporting Information), where α could be extracted. Figure 3b plots the IQE of all the measured devices, showing much weaker dependence on thickness. At low laser power (1.2 μW μm^{-2}), IQE could reach as high as 3.4×10^7 in few-layer devices.

We note that the IQE also takes into account the photoconductive gain effect. In sensitized phototransistors as demonstrated here, IQE is related to the photoconductive gain and the interfacial charge transfer efficiency by $\mathrm{IQE} = \eta_{trans} G_{ph}$ (note that η_{trans} is referred to as the IQE in some literatures[21]). We further investigate both quantities as a function of C_8-BTBT thickness (Figure 3c,d). The photoconductive gain can be derived as $G_{ph} = \tau/\tau_{transit}$, where τ is the lifetime of a charge residing on C_8-BTBT layers (the time needed for I_{ph} to drop to its $1/e$ in the recombination process), and $\tau_{transit} = L^2/(\mu V_{ds})$ is the drift transit time of electrons across graphene channel.[21,26] Despite the large scatter of data points (presumably due to the fact that the number of layers does not reflect the film morphology), we still observe an exponential increase of G_{ph} as a function of C_8-BTBT thickness (Figure 3c). This is due to the exponentially longer lifetime in thicker samples (**Figure 4**). For the monolayer and few-layer C_8-BTBT OPTs, the highest G_{ph} is 1.6×10^8 and 1.84×10^9, respectively. On the contrary, η_{trans} shows a dramatic decrease as a function of C_8-BTBT thickness (Figure 3d). This

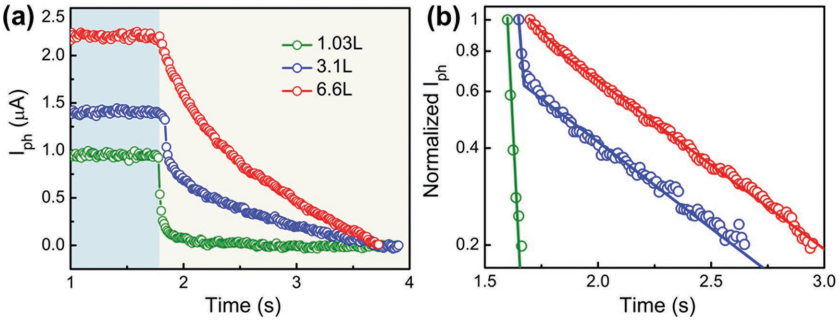

Figure 4. Response time of hybrid C_8-BTBT/graphene phototransistors. a) Measured dynamic photocurrent response of the same device in Figure 2 when the laser was turned off. Green, blue, and red symbols denote 1.03L, 3.1L, and 6.6L of C_8-BTBT, respectively. Dramatic difference in the response time can be observed. b) Logarithmic plot of the normalized photocurrent (symbols). Solid lines are exponential fitting results.

Adv. Mater. 2016,
DOI: 10.1002/adma.201600400

is not surprising because the built-in field is strongest at the C_8-BTBT–graphene interface. Nevertheless, the highest η_{trans} in few-layer C_8-BTBT devices is ≈41% (under laser power of 1.2 μW cm^{-2}), which is comparable to the best quantum dots/graphene hybrid phototransistors and MoS_2/graphene vertical photodetectors.[21,28]

The increase of R in thicker C_8-BTBT devices is accompanied by longer response times, as shown in Figures 2b and 4. We find that the charge separation process (when laser is turned on) is less affected (Figure 2b). This is because the interfacial built-in field facilitates the charge separation, thus the dynamic response is mainly limited by the recombination process. For the 1.03L and 6.6L C_8-BTBT devices in Figure 2, the response can be fitted by a single exponential decay with $\tau \approx 25$ and ≈830 ms, respectively (Figure 4b). In monolayer devices, the lifetime of trapped carriers is short because the energy barrier width for recombination is very thin (≈0.5 nm, the thickness of IL). In thicker devices, the lifetime is dominated by interlayer hopping of trapped carriers within C_8-BTBT crystals. Interestingly, in the 3.1L device where 1L and thicker layers have comparable contribution to the photoresponse, we can observe both fast and slow components (Figure 4b). We note that the slow-decaying lifetime observed in few-layer samples is comparable to previously reported solution-processed OSC/graphene hybrid phototransistors, which are also likely limited by charge transport within OSCs.[7,9] Compared to the recently reported solution-processed C_8-BTBT thin-film OPTs,[29] the maximum gain in our devices is over two orders of magnitude higher, due to the much faster transient time in graphene. The intrinsic response time of our monolayer and few-layer C_8-BTBT hybrid OPTs is four and two orders of magnitude faster, respectively, than that of C_8-BTBT thin-film OPTs (the intrinsic response time of C_8-BTBT thin-film OPTs without applying pulse gate voltage is hundreds of seconds).

The high η_{trans} and G_{ph} in our epitaxial organic crystal/graphene phototransistors can be attributed to several important factors. In organic materials, excitons have many competing relaxation pathways after initial diffusion, including ionization (electron–hole separation), trapping, exciton–exciton interactions (fission/fusion), and radiative recombination.[5] In our case, previous works have shown that the C_8-BTBT layers on graphene are highly crystalline with very low density of defects and domain boundaries. The C_8-BTBT/graphene interface is also pristine with minimum impurities.[13] Therefore, the excitons in C_8-BTBT are likely delocalized[14] and can easily diffuse to the interface with minimum trapping. This is in clear contrast with organic thin films, where disorders can strongly trap the excitons, leading to low η_{trans} and long response time. Furthermore, the high mobility in graphene ensures efficient transport of carriers to the contacts with short $\tau_{transit}$ on the order of 1 ns.

In conclusion, we have fabricated ultrathin epitaxial organic crystal/graphene hybrid structure for highly efficient phototransistors. The devices exhibit strong photoresponse down to the limit of monolayer organic semiconductors, with responsivity higher than 10^4 A W^{-1}, response time of ≈25 ms, and photoconductive gain over 10^8. Thicker organic crystals afford higher responsivity and EQE but at the price of bandwidth due to the much slower charge transport in OSCs. The excellent performance of the phototransistors is attributed to the high quality of organic crystal and interface, which is a unique feature of vdW epitaxy. Given the large library of organic molecules, we believe that epitaxial ultrathin organic crystals on graphene can serve as a versatile platform for high-performance, broadband phototransistors.

Supporting Information

Supporting Information is available from the Wiley Online Library or from the author.

Acknowledgements

X.L., X.L., and H.N. contributed equally to this work. The authors thank Nippon Kayaku Co., Ltd. Japan for providing the C_8-BTBT materials. This work was supported in part by National Key Basic Research Program of China (2013CBA01604, 2013CB932900 and 2015CB921600); National Science Foundation of China (61325020, 61261160499, 11274154, 61521001, 11574136, and 61575153); Research Grant Council of Hong Kong SAR (N_CUHK405/12); MICM Laboratory Foundation (9140C140105140C14070), a project funded by the Priority Academic Program Development of Jiangsu Higher Education Institutions, "Jiangsu Shuangchuang" program, and "Jiangsu Shuangchuang Team" Program.

Received: January 22, 2016
Revised: March 24, 2016
Published online:

[1] K.-J. Baeg, M. Binda, D. Natali, M. Caironi, Y.-Y. Noh, *Adv. Mater.* **2013**, *25*, 4267.
[2] H. L. Dong, H. Zhu, Q. Meng, X. Gong, W. P. Hu, *Chem. Soc. Rev.* **2012**, *41*, 1754.
[3] Y.-J. Cheng, S.-H. Yang, C.-S. Hsu, *Chem. Rev.* **2009**, *109*, 5868.
[4] C. L. Wang, H. L. Dong, W. P. Hu, Y. Q. Liu, D. B. Zhu, *Chem. Rev.* **2012**, *112*, 2208.
[5] C. J. Bardeen, *MRS Bull.* **2013**, *38*, 65.
[6] T. M. Clarke, J. R. Durran, *Chem. Rev.* **2010**, *110*, 6736.
[7] S.-Y. Chen, Y.-Y. Lu, F.-Y. Shih, P.-H. Ho, Y.-F. Chen, C.-W. Chen, Y.-T. Chen, W.-H. Wang, *Carbon* **2013**, *63*, 23.
[8] W.-C. Tan, W.-H. Shih, Y. F. Chen, *Adv. Funct. Mater.* **2014**, *24*, 6818.
[9] E. H. Huisman, A. G. Shulga, P. J. Zomer, N. Tombros, D. Bartesaghi, S. Z. Bisri, M. A. Loi, L. J. A. Koster, B. J. van Wees, *ACS Appl. Mater. Interfaces* **2015**, *7*, 11083.
[10] P.-H. Ho, S.-S. Li, Y.-T. Liou, C.-Y. Wen, Y.-H. Chung, C.-W. Chen, *Adv. Mater.* **2015**, *27*, 282.
[11] P.-H. Ho, C.-H. Chen, F.-Y. Shih, Y.-R. Chang, S.-S. Li, W.-H. Wang, M.-C. Shih, W.-T. Chen, Y.-P. Chiu, M.-K. Li, Y.-S. Shih, C.-W. Chen, *Adv. Mater.* **2015**, *27*, 7809.
[12] Q. L. Bao, H. Zhang, J.-X. Yang, S. W, D. Y. Tang, R. Jose, S. Ramakrishna, C. T. Lim, K. P. Loh, *Adv. Funct. Mater.* **2010**, *20*, 782.
[13] D. W. He, Y. H. Zhang, Q. S. Wu, R. Xu, H. Y. Nan, J. F. Liu, J. J. Yao, Z. L. Wang, S. J. Yuan, Y. Li, Y. Shi, J. L. Wang, Z. H. Ni, L. He, F. Miao, F. Q. Song, H. X. Xu, K. Watanabe, T. Taniguchi, J.-B. Xu, X. R. Wang, *Nat. Commun.* **2014**, *5*, 5162.
[14] Y. H. Zhang, J. S. Qiao, S. Gao, F. R. Hu, D. W. He, B. Wu, Z. Y. Yang, B. C. Xu, Y. Li, Y. Shi, W. Ji, P. Wang, X. Y Wang, M. Xiao, H. X. Xu, J.-B. Xu, X. R. Wang, *Phys. Rev. Lett.* **2016**, *116*, 016602.

[15] H. Minemawari, T. Yamada, H. Matsui, J. Tsutsumi, S. Haas, R. Chiba, R. Kumai, T. Hasegawa, *Nature* **2011**, *475*, 364.
[16] Q. L. Bao, K. P. Loh, *ACS Nano* **2012**, *6*, 3677.
[17] T. Mueller, F. N. Xia, P. Avouris, *Nat. Photonics* **2010**, *4*, 297.
[18] F. N. Xia, T. Mueller, Y.-M. Lin, A. Valdes-Garcia, P. Avouris, *Nat. Nanotechnol.* **2009**, *4*, 839.
[19] M. Freitag, T. Low, F. N. Xia, P. Avouris, *Nat. Photonics* **2013**, *7*, 53.
[20] Y. J. Zheng, Y. L. Huang, Y. F. Chen, W. J. Zhao, G. Eda, C. D. Spataru, W. J. Zhan, Y.-H. Chang, L.-J. Li, D. Z. Chi, S. Y. Quek, A. T. S. Wee, *ACS Nano* **2016**, *10*, 2476.
[21] G. Konstantatos, M. Badioli, L. Gaudreau, J. Osmond, M. Bernechea, F. P. G. de Arquer, F. Gatti, F. H. L. Koppens, *Nat. Nanotechnol.* **2012**, *7*, 363.
[22] Y. S. Wang, Y. P. Zhang, Y. Lu, W. D. Xu, C. Y. Chen, H. Qiao, J. C. Song, S. J. Li, B. Q. Sun, Y.-B. Cheng, Q. L. Bao, *Adv. Opt. Mater.* **2015**, *3*, 1389.
[23] H. Qiao, J. Yuan, Z. Q. Xu, C. Y. Chen, S. H. Lin, Y. S. Wang, J. C. Song, Y. Liu, Q. Khan, H. Y. Hoh, C. X. Pan, S. J. Li, Q. L. Bao, *ACS Nano* **2015**, *9*, 1886
[24] K. H. Kim, S. Y. Bae, Y. S. Kim, J. A. Hur, M. H. Hoang, T. W. Lee, M. J. Cho, Y. Kim, M. Kim, J.-I. Jin, S.-J. Kim, K. Lee, S. J. Lee, D. H. Choi, *Adv. Mater.* **2011**, *23*, 3095.
[25] C. R. Dean, A. F. Young, I. Meric, C. Lee, L. Wang, S. Sorgenfrei, K. Watanabe, T. Taniguchi, P. Kim, K. L. Shepard, J. Hone, *Nat. Nanotechnol.* **2010**, *5*, 722.
[26] F. H. L. Koppens, T. Mueller, Ph. Avouris, A. C. Ferrari, M. S. Vitiello, M. Polini, *Nat. Nanotechnol.* **2014**, *9*, 780.
[27] W. J. Zhang, C.-P. Chuu, J.-K. Huang, C.-H. Chen, M.-L. Tsai, Y.-H. Chang, C.-T. Liang, Y.-Z. Chen, Y.-L. Chueh, J.-H. He, M.-Y. Chou, L.-J. Li, *Sci. Rep.* **2014**, *4*, 3826.
[28] W. J. Yu, Y. Liu, H. L. Zhou, A. X. Yin, Z. Li, Y. Huang, X. F. Duan, *Nat. Nanotechnol.* **2013**, *8*, 952.
[29] Y. B. Yuan, J. S. Huang, *Adv. Opt. Mater.* **2016**, *4*, 264.

Adv. Mater. **2016**,
DOI: 10.1002/adma.201600400